Methyl Fluorocarbonyl Disulfide (FC(O)SSMe): A Theoretical Study on the Structural and Conformational Properties of Its Neutral Ground State and Lowest-Lying Cationic State

by **Mauricio F. Erben**[a])[1]) and **Carlos O. Della Védova***[a])[b])[2])

[a]) CEQUINOR (CONICET-UNLP). Departamento de Química, Facultad de Ciencias Exactas, Universidad Nacional de La Plata, 47 esq. 115 (1900) La Plata, República Argentina C.C. 962

[b]) Laboratorio de Servicios a la Industria y al Sistema Científico (LaSeISiC) (UNLP-CIC-CONICET), Camino Centenario e/505 y 508 (1897) Gonnet, República Argentina (phone/fax: +54-(0)221-4259485; e-mail: carlosdv@quimica.unlp.edu.ar)

In this work, we present a theoretical study on the structural and conformational properties of FC(O)SSMe in its neutral and cationic ground states. The structure of the neutral molecule, as deduced from *Hartree–Fock* (*HF*), *Density Functional Theory* (*DFT*), and *Møller–Plesset* (*MP2*) methods, agrees with the experimentally determined value for the CSSC dihedral angle (C–S bonds *gauche* with respect to each other) and with the *syn* preference of the SSCO dihedral angle (C=O bond *syn* with respect to the S–S bond). The calculated values for these two dihedral angles are 81.9 and 4.2 degrees, respectively. From the energy difference of the *anti vs. syn* conformer computed at the *CCSD(T)/6-311++G*** level of theory, a 3% contribution of a less-stable conformer at room temperature is proposed. The potential barrier of rotation about the S–S bond is 5.7 kcal/mol (*B3PW91/6-311++G*** approximation). The FC(O)SSMe molecule adopts a planar structure after ionization, the *anti* conformer (CSSC dihedral angle 180°) being the most-stable form. For the first ionization of the title compound, the *adiabatic* ionization potential (IP^{ad}) derived from the three mentioned theoretical methods (using the *6-311++G*** basis sets) is 8.48, 9.06, and 8.99 eV, whereas the *vertical* ionization potential (IP^{ver}) is 8.96, 9.79, and 9.62 eV, respectively (experimental value: 9.0 eV).

The results are compared with previous experimental studies carried out for the neutral and charged species interpreted on the basis of the *Natural Bond Orbital* (*NBO*) analysis. From these calculations, the importance of the anomeric and mesomeric effects becomes evident. The preferred conformation can be quantitatively explained by evaluation of donor/acceptor interaction energies.

1. Introduction. – Considerable attention has been paid in recent times to the structure and conformational preferences of simple alkyl disulfides. Since the tertiary structure of proteins is determined to a large extent by the structural properties of disulfide bridges, such compounds can serve as models for probing selected structural features of protein conformation. The minimum-energy conformation of noncon-strained, symmetrically substituted disulfides has been established both experimentally and theoretically, the value of the CSSC dihedral angle (δ(CSSC)) being close to 90° [1]. For example, dihedral angles in symmetric disulfides are 90.6(5)° (H_2S_2) [2], 87.7(4)° (S_2F_2) [3], 85.2(2)° (Cl_2S_2) [4], 85.3(37)° ($Me_2)_2S_2$) [5], and 104.4(40)° ($(CF_3)_2S_2$) [6]. However, studies on the structure elucidation and conformational behavior of non-alkyl-substituted disulfides are less common, both experimental and

[1]) This work is part of the Ph.D. thesis of *M. F. E.*

[2]) Member of CONICET, Republica Argentina.

theoretical data being scarce for these systems. Only very recently, a complete experimental study on the structure of $FC(O)SSCF_3$ was published [7].

Studies on the energy of small amino acid ions have recently been reported [8], providing a basis for the understanding of the complexities of intramolecular interactions in these systems. Reported conformation-dependent energy differences were associated with drastic changes in H-bonding upon amino acid ionization. This process is important, since charged amino acids are ubiquitous in many proteins. Their electrostatic interactions affect both structure and function [8]. On the other hand, it is evident that, due to the ease with which disulfides are oxidized to cations, the knowledge of the energetic profile of disulfide ions will lead to an improved understanding of the factors that influence and, ultimately, control the conformational flexibility and reactivity of macromolecules containing disulfide bonds [9]. One of the striking differences between the neutral molecule and the corresponding ion is the geometry of the most-stable structures. Dimethyl disulfide, $(Me)_2S_2$, has a dihedral angle of 85.3° [5][10], but the most-stable form of $(Me)_2S_2^+$ has a dihedral angle of 180°, as predicted by early semi-empirical calculations [11] and confirmed by recent high-level calculations and experimental studies [12]. Such behavior was also found in peroxides, hydrazines, and other disulfides and constitutes a typical 2-center-3-electron-π-bond system. The change in dihedral angle is evident mainly in the first band of the HeI photoelectron spectrum (PES), which is broad, unstructured, and which rises very slowly [13]. A similar change was also observed recently for the ionization of the $MeSSCH_2$ radical [14].

In previous work [15–17], we synthesized FC(O)SSMe and studied its conformational behavior by vibrational techniques (vapor and matrix IR, as well as liquid *Raman* spectroscopy) and by microwave spectroscopy. These results suggested the preference of the *syn* form for the δ(SSCO) dihedral angle with a characteristic *gauche* conformation with respect to δ(CSSC). The PES was also measured and the bands assigned with the help of the *Orbital Valence Green Functional* (*OVGF*) method of calculation [18]. Despite these extensive experimental data, systematic theoretical studies are not yet available for this molecule.

In this work, we present a theoretical study on the conformational behavior of both neutral and charged FC(O)SSMe based on three calculation levels (*HF*, *MP2* and *DFT*). The *CCSD(T)/6-311++G*** approximation was used to determine the relative populations of the most-stable rotamers. The results are compared with the experimental data available and interpreted in terms of the *NBO* analysis. The frequencies, structural parameters, and main moments of inertia are compared with the experimental data. The torsional barrier for the conformational transition and the geometry of the corresponding transition states (TS) are calculated, and the calculated first adiabatic and vertical ionization potentials (IP) are also reported.

2. Computational Methods. – All calculations have been performed with the *Gaussian98* package [19]. Levels of theory [20] employed include the use of *Self Consistent Field* (*SCF*), the second-order perturbation theory of *Møller* and *Plesset* (*MP2*) [21], and *Density Functional Theory* (*DFT*) methods [22]. The density functional applied is the three-parameter hybrid method of *Becke*, containing the *Slater* exchange term, *HF* (*Hartree–Fock*), and *Beckes* gradient correction [23], and is

combined with the correlation functional of *Perdew* and *Wang* (*B3PW*) [24]. Also, we made a single-point calculation with the single- and double-coupled cluster approach, including a perturbative estimation of connected triple excitations (*CCSD(T)*) [25]. The projected $\langle S^2 \rangle$ (spin operator) values for the unrestricted (*UHF* and *UB3PW91*) wave functions, typically 0.753, suggest that the cationic form does not present significant spin-contamination effects. The expected value for $\langle S^2 \rangle$ is 0.75 for a pure *doublet*.

Standard *Gaussian* basis sets have been used [26]. While the potential-energy surface was scanned with the *6-31G* basis set, the energy of the conformers and torsional barriers were calculated with the more-extended *6-31++G*** and split valence *6-311++G*** basis sets that include a polarized basis set and diffuse functions on both heavy and H-atoms. To reduce computational costs, the medium-size *6-31+G** basis set was used to perform the *NBO* analysis and to calculate the potential curves.

Vibrational-frequency calculations for ground and transition states have been carried out to test stationary points. To find the TS, the *Synchronous Transit-guided Quasi-Newton* (*STQN*) method implemented by *Schlegel* [27] was applied, and torsional barrier heights were calculated from the relative energies of the TS and the stable structures, taking into account the zero-point energies of the species. The hybrid functional methods have been shown to predict very well TS geometries and rotational barriers [28]. All the computed TS structures show only one imaginary frequency, which corresponds to the torsion involved in the conformational transition.

In addition, the energy differences (ΔE) calculated by the *HF*, *B3PW91*, and *MP2* methods for the first adiabatic ionization energies were obtained from the computed energy differences of FC(O)SSMe and FC(O)SSMe$^+$ at their respective minimum-energy geometries. The first vertical ionization energy was similarly obtained from single-point calculations using the computed minimum energy geometry of the neutral species.

3. Results. – We performed a scan of the energy surface by varying simultaneously the δ(SSCO)and the δ(CSSC) dihedral angles at the *HF/6-31G* level of approximation to find possible minima (*Fig. 1*). From this two-dimensional scan of the energy surface, only the mentioned *syn* and *anti* forms represent minima. Two minima with the same energy have been calculated upon varying δ(CSSC), corresponding to the helical conformations characterized by δ(CSSC) of *ca.* $+80$ and -80 degrees (enantiomers). The ball-and-stick representations of the *syn* and *anti* forms are shown in *Fig. 2* (trivial atom numbering). Relative energies of the two forms obtained with large basis sets are listed in *Table 1*. Structural properties derived from the *HF*, *B3PW91*, and *MP2* (*6-311++G***) methods for the *syn* form are listed in *Table 2*. In order to explain the *syn*/*anti* conformational preference, we performed the *NBO* analysis (*HF/6-31+G**) and evaluated the donor/acceptor energy interaction between the orbitals affected by the rotational isomerism with respect to the δ(SSCO) dihedral angle. Thus, the interactions of the two S-atom lone pairs (lpσ and lpπ) with the vicinal σ^* bond (anomeric effect) and π^* bonds (resonance or conjugation) were evaluated. The interaction of the F-atom lone pair (lpσ) with the vicinal σ^* S–C(2) bond was also computed. These results are shown in *Table 3*.

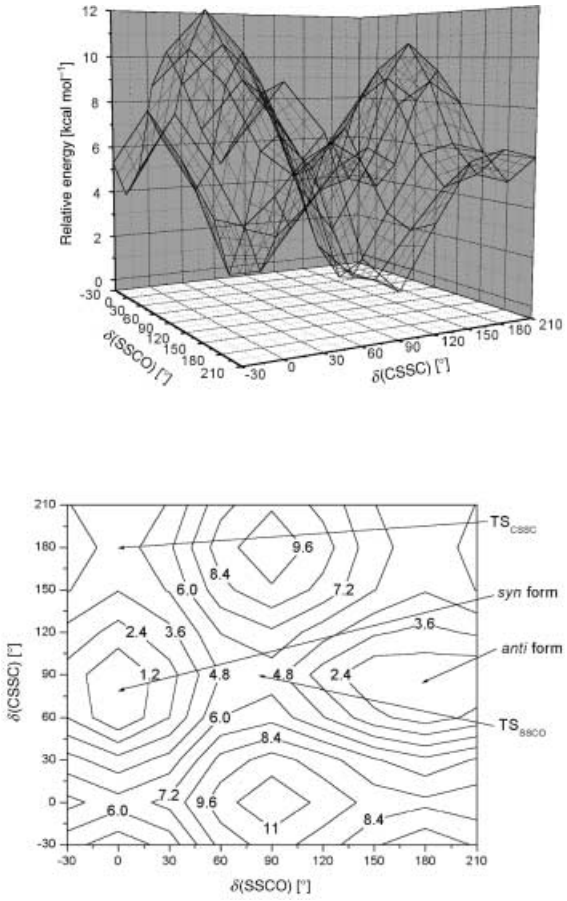

Fig. 1. *Potential-energy surface* (left) *and isoenergetic contour curve* (right) *of FC(O)SSMe as a function of the SSCO and CSSC dihedral angles calculated with the* HF/6-31G *method*

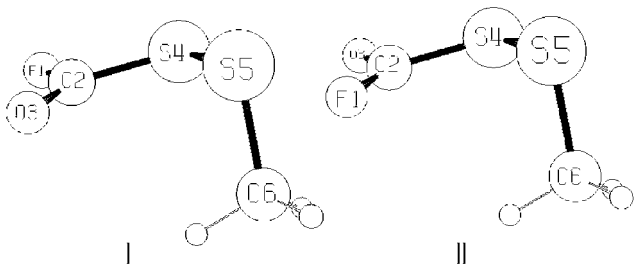

Fig. 2. *Schematic representation of the* syn (I) *and* anti (II) *conformers of FC(O)SSMe* (trivial atom numbering)

Table 1. *Calculated Relative Energies* (in kcal/mol) *for the* syn *and* anti *Conformers and Corresponding Transition States* (TS) *of Neutral FC(O)SSMe Relative to the* syn-anti, anti-anti, syn-syn, *and* anti-syn *Conformers of the Cationic Form*

FC(O)SSMe		*HF*		*B3PW91*		*MP2*	
		*6-31++G***	*6-311++G***	*6-31++G***	*6-311++G***	*6-31++G***	*6-311++G***
Neutral form	*syn*	0	0	0	0	0	0
	anti	1.82	1.74	1.45	1.48	2.29	2.16
	TS_{SSCO}	7.65	7.53	8.76	8.66	8.71	8.50
	TS_{CSSC}	5.94	5.76	5.74	5.67	6.84	6.91
Cationic form	*syn-anti*	0	0	0	0	0	0
	anti-anti	2.57	2.45	1.60	1.56	2.00	2.02
	syn-syn	4.38	4.35	3.92	3.86	4.43	4.30
	anti-syn	8.32	8.08	6.50	6.21	6.52	6.27

Table 2. *Experimental and Calculated Geometric Parameters*[a]), *Main Moments of Inertia* (*A*, *B*, *C*)[b]), *and Dipole Moments* (μ)[c]) *for the* syn *Conformer of FC(O)SSMe* (deduced by microwave spectroscopy, *HF*, *B3PW91*, and *MP2* quantum-chemical methods using the *6-311++G*** basis set)

	HF	*B3PW91*	*MP2*	Exper.[d])
C–F	1.313	1.352	1.357	1.346
C=O	1.158	1.178	1.187	1.180
S–C(2)	1.772	1.779	1.769	1.767
S–S	2.059	2.067	2.062	2.035
S–C(6)	1.814	1.817	1.805	1.810
$(C-H)_{av}$[e])	1.080	1.090	1.091	1.035
F–C=O	122.4	122.5	122.3	124.0 ± 5.0
S–C=O	129.7	130.6	130.3	130.5 ± 1.0
S–S–C(2)	102.5	102.2	100.0	97.6 ± 1.5
S–S–C(6)	102.3	102.1	100.5	108.2 ± 1.0
$(S-C-H)_{av}$[e])	109.1	110.3	109.4	109.5
δ(S–S–C=O)	−5.42	−4.2	−4.7	–
δ(C–S–S–C)	80.5	81.9	76.5	83.5 ± 1.5
A	4.743	4.6597	4.553	4.631(7)
B	1.471	1.4459	1.522	1.504(1)
C	1.282	1.2652	1.307	1.300(2)
μ	2.74	2.78	2.83	–

[a]) Distances in Å, angles in degrees. For atom numbering, see *Fig. 2*. [b]) GHz. [c]) Debye. [d]) Plausible structure of FC(O)SSMe from [17]. [e]) av: average.

Table 3. *Interaction Energies* (in kcal/mol) *for Donor/Acceptor Orbital Interactions in* syn *or* anti *Conformers and Relative Total Energies of FC(O)SSMe Using the* HF/6-31 + G* *Approximation*

	syn	*anti*
$lp_{\pi}54 \rightarrow \pi^*C=O$	37.4	33.6
$lp_{\sigma}54 \rightarrow \sigma\sigma^*C=O$	7.8	–
$lp_{\sigma}54 \rightarrow \sigma^*C-F$	–	5.1
$lp_{\pi}(4) \rightarrow \sigma^*S-C(6)$	5.5	5.8
$lp_{\sigma}F \rightarrow \sigma^*S-C(2)$	7.1	10.2
$lp_{\pi}S(5) \rightarrow \sigma^*S-C(2)$	9.3	10.7
E^{int}_{anom}	29.8	31.7
E^{int}_{conj}	37.4	33.6
ΔE_{NBO}	1.9	0.0
$\Delta E_{(anti\text{-}syn)}$	0.0	1.9

In *Table 4*, the harmonic frequencies calculated with the *HF*, *B3PW91*, and *MP2* methods using the *6-311 ++ G*** basis set for both conformers are listed together with those experimentally determined from IR and *Raman* spectra.

The potential curve obtained by variation of the δ(CSSC) dihedral angle in steps of 30° (all other parameters being optimized) at the *HF/6-31 + G** level is shown in *Fig. 3*. We performed further calculations at the *HF*, *B3PW91*, and *MP2* levels of approximation with the more-extended *6-311 ++ G*** basis sets for the *syn* and *anti* TS of FC(O)SSMe (F(O)C–S bond *syn* and *anti* with respect to the S–CH_3 bond). The *syn* form did not give rise to a plausible TS, possibly due to steric interaction between the Me and C(O)F moieties.

In order to find the TS for the *syn*/*anti* equilibrium, we also calculated the potential curve (*HF/6-31 + G**) upon varying δ(SSCO) as above and optimized the structure corresponding to the top barrier according to the *HF*, *B3PW91*, and *MP2* methods using the *6-311 ++ G*** basis sets. The potential curve is shown in *Fig. 4*. In *Table 1* and *Appendix 1*, the energy and the fully optimized geometries of these transition states are given, respectively.

Table 4. *Experimental and Theoretical Vibrational Data and Assignment of the Vibrational Modes for FC(O)SSMe*[a])[b])

Mode	*HF/6-311 ++ G***[c])		*B3PW91/6-311 ++ G***		*MP2/6-311 ++ G***		IR (gas)	*Raman* (liq.)	Assignment
	syn	*anti*	*syn*	*anti*	*syn*	*anti*			
ν_1	2971(5)	2967(6)	3165(2)	3163(3)	3201(2)	3201(0.3)	3001*w*	3002*p*	νas_{C-H}
ν_2	2954(5)	2953(5)	3147(2)	3146(2)	3188(2)	3188(2)	2928*m*	2926*p*	νas_{C-H}
ν_3	2876(20)	2875(20)	3055(11)	3054(11)	3088(12)	3088(13)			νs_{C-H}
ν_4	1860(408)		1899(323)		1861(251)		1833 *syn*, *s*	1808*p*	$\nu_{C=O}$
		1850(649)		1878/(470)		1843(394)	1781 *anti*, *m*	1768	
ν_5	1439(10)	1436(11)	1467(12)	1465(13)	1481(9)	1480(10)	1431*m*	1429	δas_{CH}
ν_6	1424(12)	1424(9)	1451(15)	1451(12)	1465(12)	1466(9)	1317		δas_{CH}
ν_7	1338(5)	1340(7)	1355(1)	1356(1)	1404(1)	1406(2)	1231*w*		δs_{CH}
ν_8	1103(563)		1047(484)		1053(455)		1050 *syn*, *vs*	ν_{C-F}	
		1130(357)		1081(344)		1074(310)	1077 *anti*, *m*		
ν_9	973(15)	971(10)	986(32)	954(13)	1017(32)	1018(5)	964*m*	958*p*	ρs_{CH}
ν_{10}	965(1)	964(0.5)	981(4)	979(2)	1009(26)	1007(10)			ρas_{CH}
ν_{11}	753(43)	752(57)	746(29)	743(37)	752(16)	750(1)	738*m*	734*p*	$\delta_{F-C=O}$
ν_{12}	680(4)	681(4)	703(2)	702(2)	748(12)	743(43)		695	ν_{H_3C-S}
ν_{13}	653(25)	651(25)	646(10)	644(11)	653(9)	647(10)	639*m*	639	oop $_{F-C=O}$
ν_{14}	523(1)	526(0.4)	527(1)	521(1)	543(1)	541(1)	537*vw*	535*p*	ν_{S-S}
ν_{15}	493(6)		492(1)		510(2)		496*vw*	512*p*, *syn*	$\nu_{F(O)C-S}$
		461(11)		465(6)		479(7)		497*p*, *anti*	
ν_{16}	352(1)	368(1)	357(1)	372(0.5)	370(1)	385(0.5)		377*p*	$\rho_{F-C=O}$
ν_{17}	242(0.5)	231(0.6)	245(0.5)	242(0.5)	260(0.4)	256(0.4)		242	ρ_{S-SCH}
ν_{18}	194(2)	194(2)	196(1.5)	196(2)	224(1)	224(1)		187	τ_{S-CH}
ν_{19}	158(1)	159(1)	159(1)	159(1)	179(2)	180(1)			δ_{FC-S-S}
ν_{20}	83(1)	77(2)	87(0.5)	81(2)	94(2)	94(2)			$\tau_{FC(O)-S}$
ν_{21}	55(3)	55(0.5)	68(3)	62(0.5)	89(0.3)	69(0.3)			τ_{S-S}

[a]) Wavenumbers in cm^{-1}, IR intensities in K $mmol^{-1}$ in parentheses. [b]) *vs:* very strong, *s:* strong, *m:* medium, *w:* weak, *vw:* very weak, *p:* polarized; ν, δ, τ, and ρ: stretching, deformation, torsion, and rocking modes, resp.; oop: out of plane. [c]) Scaled by the factor 0.90.

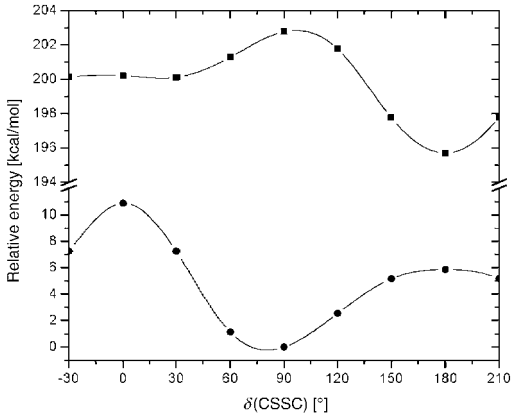

Fig. 3. *Potential-energy curves for the neutral* (●) *and cationic* (■) *forms of FC(O)SSMe as a function of the CSSC dihedral angle calculated at the* HF/6-31 + G* *level*. The SSCO dihedral angle was set to 0°.

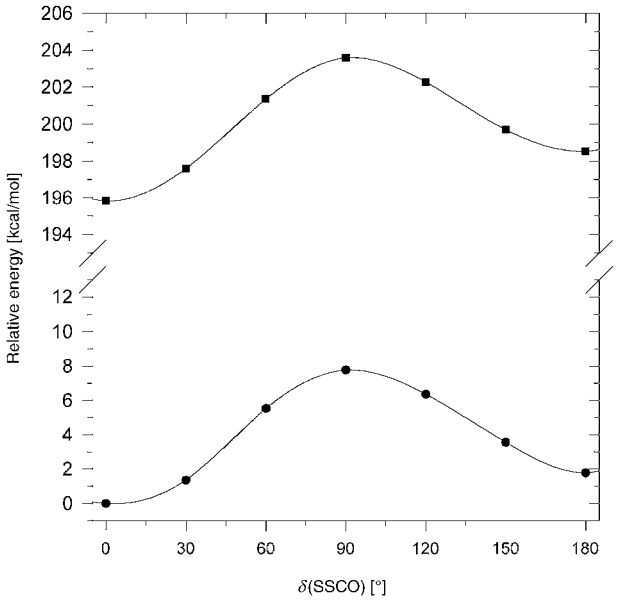

Fig. 4. *Potential-energy curves for the neutral* (●) *and cationic* (■) *forms of FC(O)SSMe as a function of the SSCO dihedral angle calculated at the* HF/6-31 + G* *level*. The SCCS dihedral angle was set to 180° for the cation.

In contrast to the neutral form, the potential curve obtained for varying δ(CSSC) of the charged form shows two minima at *ca.* 180 and 20 degrees (*Fig. 3*). The corresponding curve for the SSCO dihedral angle of the charged form is shown in *Fig. 4*. From these curves, four charged conformers are expected to be stable. The relative energies for these conformers are give in *Table 1*. The geometric parameters

and fundamental vibrational frequencies for the most-stable *syn*/*anti* conformer obtained at the *HF* and *B3PW91* (*6-311++G***) levels are listed in *Appendices 2* and *3*, respectively.

4. Discussion. – 4.1. *Neutral Form of Methyl Fluorocarbonyl Disulfide.* 4.1.1. *Equilibrium geometry.* For the reported microwave spectrum of FC(O)SSMe, only transitions for the *syn* conformer were assigned, and several geometric parameters had to be assumed [17]. Vibrational spectra confirm this result and indicate the presence of a second conformer. The calculated (*B3PW91/6-311++G***) free-enthalpy difference ($\Delta G^\circ = 1.40$ kcal/mol) corresponds to a *syn*/*anti* ratio of 91:9. This relatively high concentration of the *anti* form at room temperature cannot be derived from the reported IR spectra because the $\nu_{C=O}$ stretching mode assigned to the *anti* form is presumably masked by a $\nu_{C-F} + \nu a_{C-S}$ combination mode. As a further test, we performed a *CCSD(T)/6-311++G*** energy calculation for both the *syn* and *anti* conformers (the geometry being taken from the *MP2/6-311++G*** output file). A ΔE value of 2.03 kcal/mol was computed, which corresponds to a contribution of only 3% for the less-stable form at 298 K. However, although the determination of the *syn*/*anti* ratio is not feasible from IR spectra, a higher contribution of the *anti* form should be expected according to the experimental spectra [17] and from the calculated intensities listed in *Table 4*. Thus, the experimental values seem to be closer to the results obtained from the *B3PW91/6-311++G*** model. The calculated geometrical parameters of the *syn* form are compared to the experimental values in *Table 2*. The levels of approximation used reproduce the experimental bond lengths with an accurancy higher than 0.03 Å. The calculated bond angles also show reasonable agreement to the experimental values, except for the two SSC bond angles, which are *ca.* 4° larger and 6° smaller than the experimental values (see *Table 2*). However, the calculated SSC angles are in close agreement to the experimental values reported for the fluorinated derivative $FC(O)SSCF_3$ [7]. This might indicate that the experimentally determined bond angles in FC(O)SSMe are not very precise.

The calculated moments of inertia ($A-C$) are in close agreement to the experimental values obtained by microwave spectroscopy. The predicted values for the dipole moment are 2.74, 2.78, and 2.83 D for the *HF*, *B3PW91*, and *MP2* (*6-311++G***) methods, respectively.

As pointed out by *Oberhammer* and co-workers [7], in all disulfur compounds X–S–S–X in which X contains carbon (*e.g.*, X = FC(O), CF_3, Me), and even in $FC(O)SSCF_3$, the S–S bond length is close to 2.02 Å, whereas the S–S bond lengths for symmetrically substituted disulfur compounds are strongly influenced by the X group, with a rather large variation from 1.890(2) Å in FSSF [3] to 2.0610(3) Å in HSSH [29]. Thus, the S–S bond lengths for FC(O)SSC(O)F, CF_3SSCF_3, MeSSMe, ^{t}BuSS^{t}Bu, and $FC(O)SSCF_3$ are 2.028(4) [30], 2.030(5) [6], 2.029(3) [5], 2.018(4) [7], and 2.027(4) Å [7], respectively. The calculated value for FC(O)SSMe of *ca.* 2.06 Å is slightly larger than the value deduced from microwave spectra (2.035 Å), even when electronic correlation at the *MP2* level is taken into account (2.062 Å). However, it is important to note that the calculated S–S bond length in MeSSMe using the *B3PW91* and *MP2* methods and the *6-311++G*** basis sets are 2.073 and 2.065 Å, respectively, which is *ca.* 0.04 Å higher than the experimental value. These methods are, thus, not

powerful enough to precisely predict the S–S bond length at the above levels of approximation [10b]. Thus, the S–S bond length deduced from microwave spectra [17] for the more-plausible structure of FC(O)SSMe, although larger than the experimental values obtained for the corresponding symmetrically substituted analog, is the best description available.

4.1.2. NBO *Analysis.* The results listed in *Table 3* demonstrate that the conformational preference with respect to the δ(SSCO) dihedral angle is mainly due to mesomeric stabilization ($lp_{\pi}S(4) \rightarrow \pi^{*}C{=}O$) of the *syn* form. The anomeric effect restricted to the analysis of the conformational preference due to the relative position of the F(1)- and O(3)-atoms reinforces the mesomeric tendency ($lp_{\sigma}S(4) \rightarrow \sigma^{*}C{=}O =$ 7.8 kcal/mol for the *syn* rotamer, $lp_{\sigma}S(4) \rightarrow \sigma^{*}C{-}F = 5.1$ kcal/mol for the *anti* form). Thus, to the $37.4 - 33.6 = 3.8$ kcal/mol of stabilization caused by the mesomeric effect, the preference of the *syn* conformation adds $7.8 - 5.1 = 2.7$ kcal/mol from the anomeric effect. The overall 6.6 kcal/mol exceed the 1.9 kcal/mol calculated as the energy difference between the two rotamers (*Table 3*). Therefore, we searched for other interactions that might also contribute to the energy difference between the two forms especially, $lp_{\pi}S(4) \rightarrow \sigma^{*}S{-}C(6)$, $lp_{\sigma}F \rightarrow \sigma^{*}S{-}C(2)$ and $lp_{\pi}S(5) \rightarrow \sigma^{*}S{-}C(2)$. Thus, the total anomeric effect favored the *anti* form, as deduced from the sum of the σ sulfur ($lp_{\sigma}S(4) \rightarrow \sigma^{*}C{-}F$ and $lp_{\sigma}S(4) \rightarrow \sigma^{*}C{=}O$) and fluorine ($lp_{\sigma}F \rightarrow \sigma^{*}S{-}C(2)$) lone-pair contributions and the π anomeric interactions ($lp_{\pi}S(5) \rightarrow \sigma^{*}S{-}C(2)$ and $lp_{\pi}S(4) \rightarrow \sigma^{*}S{-}C(6)$). Therefore, the contribution of the mesomeric effect in the stabilization of the *syn* form is 3.8 kcal/mol, and the anomeric effect favors the *anti* form by 1.9 kcal/mol. The difference between the contributions of the anomeric and mesomeric effects for the two conformers ($\Delta E_{NBO} = 1.9$ kcal/mol) agrees with the total energy difference $\Delta E = E_{anti} - E_{syn} = 1.9$ kcal/mol estimated by means of the *HF/6-31 + G** approximation.

Two plausible interpretations for the preference of the XSSX dihedral angle are usually given. From a population analysis, *Boyd* [31] concluded that the repulsion of the $3p\pi$ lone pairs is minimized when these atomic orbitals (AOs) are oriented orthogonal to each other. The second argument is based on hyperconjugation, whereby the π character of the S–S bond is enhanced when the S–X bonds are aligned for maximum transfer of electron density through the $3p\pi$ AOs of the X group [1b]. This is consistent with the anomeric effect, *i.e.*, electron donation from the sulfur lone pair into the empty σ^{*} orbital of the opposite S–X bond [32]. *Fig. 5* shows the variation of the orbital interaction relevant for the conformational preference of δ(CSSC) as a function of the dihedral angle ($lp_{\pi}S(4) \rightarrow \pi^{*}C{=}O$, $lp_{\pi}S(5) \rightarrow \sigma^{*}S{-}C(2)$ and $lp_{\pi}S(4) \rightarrow \sigma^{*}S{-}C(6)$). The higher the interaction energy, the higher the stabilization energy. While the $lp_{\pi}S(4) \rightarrow \pi^{*}C{=}O$ interaction favors dihedral angles of 0° and 180° (maximum orbital overlap), the anomeric interaction of the sulfur lp_{π} orbital with the opposite $\sigma^{*}S{-}C(6)$ orbital is responsible for the preferred *gauche* conformation. These interactions can be represented by a no-bond-double-bond structure [$R{-}S{-}S{-}R \leftrightarrow R{-}S^{+}{=}S\ R^{-}$]. The sum of the relevant orbital-interaction energies has its maximum at a dihedral angle of *ca.* 85°, *i.e.*, close to the minimum of the total energy at 80.5° (see *Fig. 3*). From comparison between the total energy and the main interaction energies, it is evident that there is high steric strain in the *syn* form, which explains its high energy that cannot be explained by orbital interactions.

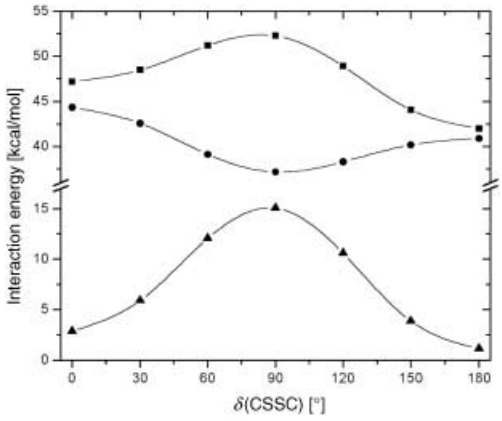

Fig. 5. *Interaction energies for the main orbitals of FC(O)SSCH$_3$ evaluated at the* HF/6-31 + G* *method, as a function of the δCSSC dihedral angle, using the* NBO *analyses* (● resonance interaction, ▲ anomeric interaction and ■ anomeric plus resonance interaction)

In order to check the NBO results, a similar analysis was performed for HSSH. The calculated $lp_{\pi}S \rightarrow \sigma^{*}S-H$ (anomeric) and $lp_{\pi}S \rightarrow RY^{*}\sigma S$ (*Rydberg*) relative interaction energies are shown in *Fig. 6*. Clearly, the anomeric effect is responsible for almost the total energy differences observed upon varying δ(HSSH). The inclusion of the main *Rydberg* interaction leads to a certain improvement, however, it is clear that other contributions, such as steric effects, must play a secondary, but important role.

4.1.3. *Vibrational Analysis.* From *Table 4*, it can be seen that the computed harmonic frequencies at both *HF* (scaled) and *B3PW91* (*6-311 ++ G***) methods are remarkably successful. The inclusion of electronic correlation through the perturbative *MP2* method leads to an acceptable agreement between the calculated harmonic and the observed fundamental frequencies without the inclusion of scaling factors. These theoretical results confirm the previous vibrational assignment of the bands [17] and support the existence of a *syn*/*anti* conformational equilibrium at room temperature, as evidenced by the $\nu_{C=O}$ and ν_{C-F} stretching and the $\rho_{F-C=O}$ rocking modes for the two conformers, which show a splitting of + 52, − 27, and + 15 cm^{-1}, respectively, and could be clearly identified. The theoretical splitting (*MP2/6-311 ++ G***), obtained from the difference between the corresponding frequencies for the *syn* and *anti* forms, is + 18, − 21, and + 31 cm^{-1} for the ν_4, ν_8, and ν_{16} fundamental modes, respectively. It should be noted that the frequency shifts follow the observed ones in the vibrational spectra.

4.1.4. *Rotational Transition States.* Even for the parent compound, H_2S_2, experimental information on the S−S torsional potential is scarce. *Redington* [33] analyzed the torsional band of H_2S_2 in the far-IR spectrum. Using a model potential, he estimated a barrier of *ca.* 6.9 kcal/mol for the transition between the enantiomeric helical conformers characterized by δ(HSSH) dihedral angles of *ca.* 90 and − 90°. This barrier could be considered as the average of the *syn* and *anti* barrier. Similarly, from the very small torsional splitting observed in the rotational spectra of the vibrational ground state, *Winnewisser* and co-workers [34] established that the barrier to internal

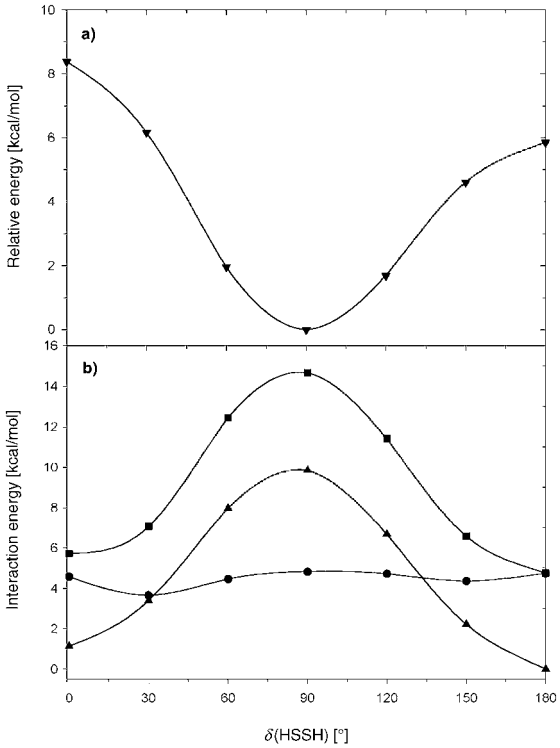

Fig. 6. a) *Relative energy of H_2S as a function of δ(CSSC) evaluated by the* HF/6-31 + G* *method*. b) *Interaction energies between the main orbitals of H_2S evaluated by the* HF/6-31 + G* *method as a function of δ(HSSH) using the* NBO *analysis* (▲ anomeric interaction, ● $lp_\pi S \rightarrow RY^*\sigma S$ *Rydberg* interaction, ■ anomeric plus *Rydberg* interaction).

rotation in H_2S_2 is much higher than that for the O–O bond in H_2O_2. However, the magnitudes of the nonequivalent *syn* and *anti* barriers have not yet been established experimentally. There have been reports of torsional barriers in H_2S_2 calculated with *ab initio* methods, with *syn* and *anti* barriers being 7.5 ± 0.15 and 5.0 ± 0.15 *vs.* 7.83 and 5.01 kcal/mol, respectively. These results take into account electronic correlation effects through *MP2* and *CI-SD* calculations [35].

The potential curve for the δ(CSSC) dihedral angle in FC(O)SSMe is shown in *Fig. 3*. From this curve, the TS structure that connects the two enantiomeric forms of the molecule results in a planar *anti* conformation ($\delta(CSSC) = 180^\circ$) with the H_3C–S bond *anti* to the S–C(O)F bond. On the other hand, the TS for rotation of the C(O)F group about the S–C(2) bond (TS_{SSCO}) possesses a *skew* structure (δ(SSCO) close to 90°).

The potential barriers to internal rotation about the S–S and S–C(2) bonds are given in *Table 1*. The *B3PW91/6-311 ++ G*** value for S–S rotation (5.67 kcal/mol) is close to the value reported by *Li et al.* [12] obtained for the C_{2h} TS of MeSSMe (5.8 kcal/mol) at the *G2(MP2)* level of theory.

The geometric parameters optimized for both transition states are listed in *Appendix 1*. Except for the dihedral angles, other parameters change with respect to the minimum conformer. Thus, the S–S bond in TS_{CSSC} is *ca.* 0.06 Å longer and the S–S–C angles are by 4–6° smaller than the corresponding values in the ground-state structure. In the TS_{SSCO}, the S–C(2) bond is lengthened by *ca.* 0.04 Å, and the S–S–C(2) angle is decreased by *ca.* 4°.

4.2. *Radical Cation of Methyl Fluorocarbonyl Disulfide.* The four stable conformers of FC(O)SSMe$^{\bullet+}$ named *syn-anti*, *anti-anti*, *syn-syn*, and *anti-syn*, depending on the mutual orientation of the C=O/S–S and H_3C–S/S–C(O)F bonds, respectively) are shown in *Fig. 7*, and their relative energies are given in *Table 1*. The two *anti* conformers with respect to the δ(CSSC) dihedral angle have a planar main-atom structure with C_S symmetry, whereas the two *syn* conformers possess C_1 symmetry. The potential curve for δ(CSSC) = 0 is very flat, and the stable structure has a δ(CSSC) close to 20° (see *Fig. 3*). From *Table 1*, the most-stable species corresponds to the *syn-anti* form. Thus, after ionization, the δ(SSCO) dihedral angle is retained, but δ(CSSC) adopts a value of 180° (structure I in *Fig. 7*). This finding is in agreement with experimental and theoretical results for MeSSMe and $MeSSCH_2$ (see *Introduction*) [14][36].

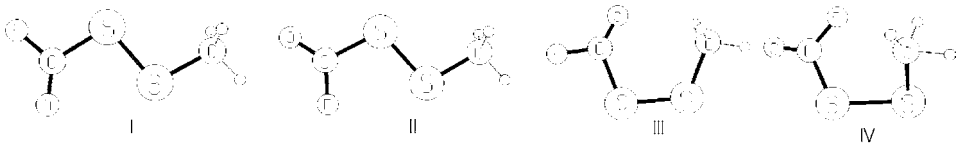

Fig. 7. *Schematic representation of the* syn-anti (I), anti-anti (II), syn-syn (III), *and* anti-syn (IV) *conformers of FC(O)SSMe*$^{\bullet+}$

The calculated geometric parameters (*UHF*, *UB3PW91*, and *UMP2/6-311++G***) for all four stable conformers are listed in *Appendix 2*. Relative to the neutral species, the S–S and C–F bonds are shortened by *ca.* 0.04 and 0.05 Å, respectively, whereas the S–C(2) bond is lengthened by 0.08 Å. The S–S–C(2) and S–C=O angles decrease by *ca.* 5–6°.

Changes in geometry are followed by changes in the fundamental frequencies. As can be seen in *Appendix 3*, the $3N - 6 = 21$ normal modes of vibration are classified as *7A″ out-of-plane* and as *14A′ in-plane* modes, as deduced from the selection rules of the C_S point group of symmetry. The more-important frequency shifts are displayed by the ν_3, ν_7 and ν_{10} modes, which correspond to the $\nu_{C=O}$, ν_{C-F} and ν_{S-S} stretching vibrations, respectively. These three modes are shifted to higher frequencies upon ionization, as expected from the shortened C=O, C–F and S–S bond lengths. These changes can be rationalized by considering that the charge is mainly localized at the S-atom bonded to the Me group and by the planar main-atom skeleton of the cation. Thus, the shortening of the S–S bond is explained by a bond reinforcement when the $lp_\pi S$ repulsion disappears and by the shortening of the bonds in the C(O)F moiety by conjugation. On the other hand, the ν_{S-CH} and $\nu_{S-C(O)F}$ stretching modes are shifted to lower frequencies. This diminution in the bond order is easily explained for the first of these modes,

because the ionization takes place mainly at the S-atom next to the Me group. The photoelectron spectrum does not allow any assignment for these vibrations [18].

Related to general FC(O)SY-containing compounds, experimental mass spectra of both neutral and charged species of FC(O)SCl and FC(O)SNCO provide evidence that, upon ionization, both the enthalpy difference between the *syn* and *anti* conformers and the barrier to internal rotation about the C–S single bond decrease [37]. In the present case, however, the barrier calculated for charged FC(O)SSMe is about the same as that of the neutral form, and the difference between the *syn* and *anti* forms is *ca.* 1 kcal/mol higher in the cation as compared to the neutral form. These opposite trends are related to the observation that in the above FC(O)SY compounds both the neutral molecule and the cation are planar, whereas, in FC(O)SSMe, a drastic change in geometry upon ionization occurs, mainly in the CSSC more than in the FC(O)S moiety.

Taking into account the energy of the most-stable *syn-anti* form of $FC(O)SSCH_3^{\bullet+}$, a value for the adiabatic ionization potential (IP^{ad}) of 9.06, 8.48, and 8.99 eV is derived from the *B3PW91*, *HF*, and *MP2* (*6-311++G***) approximations, respectively. Because of the very poor *Frank–Condon* factors for the ionization transition near the threshold displayed by several S-containing molecules, the true IP^{ad} energies could not be observed. The reported value for the vertical ionization potential (IP^{ver}) for this molecule is 9.0 eV [18]. To compare this vertical ionization energy, a calculation of the energy of the radical cation at the fixed geometry of the neutral ground state was performed. The values calculated with the above approximations are 9.79, 8.96, and 9.62 eV, respectively, in reasonable agreement with the experimental value and also with the value calculated by the (*OVGF/6-31G*) method (9.5 eV).

5. Conclusions. – FC(O)SSMe follows the same general trend observed in previous conformational studies of thioesters (–C(O)S–) and disulfides (–SS–). Several sulfenyl carbonyl compounds of the type XC(O)SY have been studied. The general tendency is the preference for the *syn* conformation (C=O bond *syn* with respect to the S–Y bond) over to the *anti* conformation. Furthermore, for FC(O)SY compounds, a minor proportion of the *anti* form seems to be in equilibrium with the *syn* conformer at ambient temperature [38]. Moreover, the structure of disulfides (XSSX) are characterized by dihedral angles δ(XSSX) close to 90°.

Molecules containing both C(O)F and S_2 moieties, such as FC(O)SSC(O)F [39] and FC(O)SSC(O)Cl [40], also prefer the *syn* conformation with respect to the SSC(O) dihedral angle, and possess C_2 and C_1 symmetry, respectively, as deduced from vibrational studies. More recently, gas electron-diffraction studies in $FC(O)SSCF_3$ resulted in δ(CSSC) and δ(SSCO) dihedral angles of 95.0(27) and 2.3° (not refined), respectively [7].

The present theoretical results confirm this strong trend for the FC(O)S-containing compounds, *i.e.*, FC(O)SSMe possesses C_1 symmetry and prefers the *syn* conformation. In the context of the *NBO* analysis, the *syn* preference can be rationalized by the large calculated difference in resonance interaction (3.8 kcal/mol) for the two forms. This difference must be emphasized because, in a first approximation, one would expect that this interaction does not depend on the conformation of this part of the molecule. This behavior was also observed in the XC(O)SCl (X = F, Cl, Br, F_3C and MeO) series [41]. The *NBO* analysis also rationalizes the *gauche* structure around the S–S bond.

Anomeric interactions between the S-atom lone pairs and opposite S–C bonds favor this structure, an analysis that also applies to H_2S_2.

A dramatic change occurs in the geometry of the molecule upon ionization: the δ(CSSC) dihedral angle adopts a value of 180°, leading to C_S molecular symmetry for the resulting cation. This geometric change between the neutral and charged forms may be the reason for the broad band observed in the first band of the photoelectron spectrum of the molecule, corresponding to an electron withdrawn from the lone pair of the S-atom attached to the Me group [18]. The calculated theoretical IP^{ad}, *ca.* 9 eV, are in the range of the values displayed by other disulfides with similar substituents, *e.g.*, 8.7 and 10.6 eV for MeSSMe and CF_3SSCF_3, respectively [42]. Similarly, the calculated IP^{ver} of *ca.* 9.6 eV is in close agreement with the experimental value obtained from photoelectron spectra (9.0 eV).

C.O.D.V. acknowledges Prof. *A. Haas* (Ruhr-Universität Bochum) and Prof. Em. *P. J. Aymonino* for their stimulating contributions. The authors also thank the *Fundación Antorchas*, *Alexander von Humboldt*, *DAAD* (Deutscher Akademischer Austauschdienst), *Agencia Nacional de Promoción Científica y Técnica* (*ANPCYT*), *Consejo Nacional de Investigaciones Científicas y Técnicas* (*CONICET*), *Comisión de Investigaciones de la Provincia de Buenos Aires* (*CICBA*), British Council, Jesus College of Oxford, and *Facultad de Ciencias Exactas* (*UNLP*) for financial support. They are indebted to the *AvH-Fundación Antorchas* and *ANPCYT-DAAD* for the German/Argentinean cooperation Awards. The authors are very grateful to Dr. *M. A. Mroginski*, Max-Planck-Institut für Strahlenchemie, Mülheim an der Ruhr, for the help on computation *CCSD(T)* energies and *MP2* frequencies.

Appendix 1. *Calculated Parameters for Conformational Transition States of FC(O)SSMe*[a])

	*HF/6-311++G***		*B3PW91/6-311++G***		*MP2/6-311++G***	
	TS_{SSCO}	TS_{CSSC}	TS_{SSCO}	TS_{CSSC}	TS_{SSCO}	TS_{CSSC}
C–F	1.308	1.312	1.343	1.351	1.349	1.356
C=O	1.159	2.158	1.179	1.181	1.189	1.189
S–C(2)	1.802	1.758	1.816	1.755	1.798	1.750
S–S	2.074	2.104	2.083	2.122	2.080	2.111
S–C(6)	1.815	1.814	1.817	1.815	1.805	1.807
$(C–H)_{av}$[b])	1.082	1.082	1.091	1.091	1.091	1.091
F–C=O	121.6	122.6	121.6	122.7	121.4	122.6
S–C=O	126.1	128.9	126.8	129.7	126.7	129.7
S–S–C(2)	98.6	98.9	97.7	97.9	95.1	97.0
S–S–C(6)	102.1	96.2	102.3	96.2	100.0	94.6
$(S–C–H)_{av}$	109.0	110.4	110.9	109.5	109.4	110.6
δ (S–S–C=O)	90.4	0.0	91.2	0.0	91.8	0.0
δ (C–S–S–C)	90.4	180.0	– 84.1	180.0	– 80.4	180.0
μ [D]	2.51	4.01	2.41	3.99	2.63	4.30

[a]) Distances in Å, bond angles and torsion angles in degrees.

Appendix 2. *Calculated Parameters for the* syn-anti, anti-anti, syn-syn, *and* anti-syn *Conformers of FC(O)SSMe*$^{\bullet+}$ [a])

	*UHF/6-311++G***				*UB3PW91/6-311++G***				*MP2/6-311++G***			
	syn-anti	*anti-anti*	*syn-syn*	*anti-syn*	*syn-anti*	*anti-anti*	*syn-syn*	*anti-syn*	*syn-anti*	*anti-anti*	*syn-syn*	*anti-syn*
C–F	1.278	1.288	1.280	1.291	1.302	1.310	1.305	1.312	1.308	1.315	1.310	1.317
C=O	1.147	1.143	1.150	1.143	1.166	1.165	1.168	1.165	1.175	1.171	1.176	1.172
S–C(2)	1.825	1.826	1.816	1.818	1.864	1.851	1.852	1.846	1.861	1.856	1.851	1.859
S–S	2.015	2.011	2.029	2.022	2.023	2.027	2.031	2.037	1.985	1.991	1.990	1.990
S–C(6)	1.824	1.823	1.830	1.828	1.809	1.810	1.806	1.807	1.806	1.806	1.803	1.805
$(C–H)_{av}$	1.081	1.081	1.080	1.080	1.092	1.092	1.092	1.091	1.901	1.092	1.091	1.091
F–C=O	127.8	127.7	127.0	127.0	128.9	128.7	127.9	128.2	129.0	128.8	128.2	128.6
S–C=O	125.1	119.4	126.7	113.8	125.2	119.0	127.4	117.5	125.4	119.4	126.6	120.7
S–S–C(2)	97.3	102.6	105.1	113.7	96.4	101.8	107.4	114.3	96.4	102.3	106.3	112.1
S–S–C(6)	100.5	100.6	112.5	111.9	100.9	101.0	112.5	112.5	99.7	99.7	111.2	109.0
$(S–C–H)_{av}$	107.6	107.5	107.0	109.2	108.4	108.3	108.0	108.0	108.3	108.1	108.1	108.4
δ(S–S–C=O)	0.0	180.0	4.1	180.0	0.0	180.0	5.6	−178.0	0.0	180.0	17.5	−12.3
δ(C–S–S–C)	180.0	180.0	27.4	27.1	180.0	180.0	12.7	4.8	180.0	180.0	17.0	−47.2

[a]) Bond lengths in Å, bond and torsion angles in degrees.

Appendix 3. *Calculated Vibrational Frequencies in cm*$^{-1}$ *for the* syn-anti C_s*-Symmetric Conformer of FC(O)SSMe*$^{\bullet+}$ *by Means of* HF *and* B3PW91 *Quantum-Chemical Approaches Using the* 6-311++G** *Basis Set* [a])

Mode	Symmetry	*HF*	*B3PW91*
ν_1	A′	3318.7 (7)	3160.4 (9)
ν_2	A′	3196.7 (10)	3048.9 (34)
ν_3	A′	2141.4 (370)	1979.5 (247)
ν_4	A′	1556.7 (10)	1426.1 (10)
ν_5	A′	1482.3 (11)	1356.2 (6)
ν_6	A′	1278.8 (677)	1129.7 (568)
ν_7	A′	1102.5 (1)	997.7 (1)
ν_8	A′	816.3 (175)	718.2 (164)
ν_9	A′	712.6 (30)	672.8 (7)
ν_{10}	A′	588.4 (37)	584.6 (10)
ν_{11}	A′	521.8 (16)	450.2 (14)
ν_{12}	A′	378.6 (3)	342.0 (0.1)
ν_{13}	A′	253.8 (6)	234.2 (3)
ν_{14}	A′	149.7 (1)	129.6 (0.6)
ν_{15}	A″	3310.0 (6)	3158.2 (9)
ν_{16}	A″	1562.8 (25)	1427.0 (26)
ν_{17}	A″	1022.4 (0.08)	939.8 (2)
ν_{18}	A″	675.3 (9)	624.9 (15)
ν_{19}	A″	133.0 (0.04)	126.7 (0.0002)
ν_{20}	A″	84.7 (0.2)	79.0 (0.2)
ν_{21}	A″	78.5 (0.02)	72.7 (0.0001)

[a]) Intensities in parentheses.

REFERENCES

[1] a) M. E. Van Wart, L. L. Shipman, H. A. Scheraga, *J. Phys. Chem.* **2000**, *79*, 1848. b) D. B. Boyd, *J. Phys. Chem.* **1974**, *78*, 1554. c) M. T. Devlin, G. Barany, I. R. Levin, *J. Mol. Struct.* **1990**, *238*, 119.
[2] G. Winnewisser, *J. Mol. Spectrosc.* **1972**, *41*, 534.
[3] C. J. Marsden, H. Oberhammer, O. Lösking, H. Willner, *J. Mol. Struct*. **1989**, *193*, 233.
[4] C. J. Marsden, R. D. Brown, P. D. Godfrey, *J. Chem. Soc., Chem. Commun*. **1979**, 399.
[5] A. Yokozeki, S. H. Bauer, *J. Phys. Chem*. **1976**, *80*, 618.
[6] C. J. Marsden, B. J. Beagley, *J. Chem. Soc., Faraday Trans. 2* **1981**, *77*, 2213.
[7] A. Hermann, S. E. Ulic, C. O. Della Védova, H.-G. Mack, H. Oberhammer, *J. Fluorine Chem.* **2001**, *112*, 297.
[8] K. T. Lee, J. Sung, K. J. Lee, Y. D. Park, S. K. Kim, *Angew. Chem., Int. Ed.* **2002**, *41*, 4114.
[9] W. J. Wedemeyer, E. Welker, M. Narayan, H. A. Scheraga, *Biochemistry* **2000**, *39*, 4207; H. Beinert, *Eur. J. Biochem.* **2000**, *267*, 5657; S. W. Bass, S. A. Evans Jr., *J. Org. Chem.* **1980**, *45*, 710.
[10] a) D. Sutter, H. Dreizler, H. D. Rudolph, *Z. Naturforsch. A* **1965**, *20*, 1676. b) M. Meyer, *J. Mol. Struct.* **1992**, *273*, 99.
[11] T. Gillbro, *Phosphorus Sulfur Relat. Elem.* **1978**, *4*, 133.
[12] W.-K. Li, S.-W. Chiu, Y.-X. Ma, C.-L. Liao, C. Y. Ng, *J. Chem. Phys.* **1993**, *99*, 8440.
[13] K. Osafune, S. Katsumata, K. Kimura, *Chem. Phys. Lett.* **1973**, *19*, 369; G. Wagner, H. Bock, *Chem. Ber*. **1974**, *107*, 68.
[14] J. Backer, J. M. Dyke, *J. Phys. Chem*. **1994**, *98*, 757.
[15] C. O. Della Védova, A. Haas, *Z. Anorg. Allg. Chem.* **1991**, *600*, 145.
[16] C. O. Della Védova, *Spectrochim. Acta, Part A* **1991**, *11*, 1619.
[17] C. Fantoni, C. O. Della Védova, *J. Mol. Spectrosc.* **1992**, *154*, 240.
[18] M. F. Erben, C. O. Della Védova, *Inorg. Chem.* **2002**, *41*, 3740.
[19] M. J. Frisch, G. W. Trucks, H. B. Schlegel, G. E. Scuseria, M. A. Robb, J. R. Cheeseman, V. G. Zakrzewski, J. A. Montgomery, R. E. Stratman, J. C. Burant, S. Dapprich, J. M. Millam, A. D. Daniels, K. N. Kudin, M. C. Strain, O. Farkas, J. Tomasi, V. Barone, M. Cossi, R. Cammi, B. Menucci, C. Pomelli, C. Adamo, S. Clifford,. J. Ochterski, G. A. Petersson, P. Y. Ayala, Q. Cui, K. Morokuma, D. K. Malick, A. D. Rabuck,. K. Raghavachari, J. B. Foresman, J. Cioslovski, J. V. Ortiz, B. B. Stefanov, G. Liu, A. Liashenko, P. Piskorz, I. Komaromi, R. Gomperts, R. L. Martin, D. J. Fox, T. Keith, M. A. Al-Laham, C. Y. Peng, A. Nanayakkara, C. Gonzales, M. Challacombe, P. M. W. Gill, B. Johnson, W. Chen, M. W. Wong, J. L. Andres, M. Head-Gordon, E. S. Replogle, J. A. Pople, GAUSSIAN98 (Revision A.7), Gaussian, Inc., Pittsburgh PA, 1998.
[20] S. Szabo, N. S. Ostlund, 'Modern Quantum Chemistry', Dover, New York, 1996.
[21] C. C. J. Roothan, *Rev. Mod. Phys.* **1960**, *32*, 179; C. Møller, M. S. Plesset, *Phys. Rev.* **1934**, *46*, 618.
[22] P. Hohenberg, W. Kohn, *Phys. Rev. B* **1964**, *136*, 864; W. Kohn, L. J. Sham, *Phys. Rev. A* **1965**, *140*, 1133.
[23] A. D. Becke, *J. Chem. Phys.* **1993**, *98*, 5648.
[24] J. P. Perdew, Y. Wang, *Phys. Rev. B* **1992**, *45*, 13244.
[25] R. J. Bartlett, *J. Phys. Chem.* **1989**, *93*, 1697.
[26] M. J. Frisch, J. A. Pople, J. S. Binkley, *J. Chem. Phys.* **1984**, *80*, 3265.
[27] C. Peng, P. Y. Ayala, H. B. Schlegel, M. J. Frisch, *Comput. Chem.* **1996**, *17*, 49.
[28] B. J. Lynch, D. G. Truhlar, *J. Phys. Chem. A* **2001**, *105*, 2936.
[29] C. J. Marsden, B. J. Smith, *J. Phys. Chem.* **1989**, *92*, 347.
[30] H.-G. Mack, C. O. Della Védova, H. Oberhammer, *J. Phys. Chem.* **1992**, *92*, 9215.
[31] D. B. Boyd, *J. Am. Chem. Soc.* **1972**, *94*, 8799; R. J. Boyd, J. S. Perkyns, R. Ramani, *Can. J. Chem.* **1983**, *61*, 1082.
[32] A. J. Kirby, 'The Anomeric Effect and Related Stereochemical Effects at Oxygen', Springer, Berlin, 1983; D. R. Alleres, D. L. Cooper, T. P. Cunningham, J. Gerratt, P. B. Karadakov, M. Raimondi *J. Chem. Soc., Faraday Trans.* **1995**, *91*, 3357.
[33] R. L. Redington, *J. Mol. Spectrosc*. **1962**, *9*, 469.
[34] G. Winnewisser, M. Winnewisser, W. Gordy, *J. Chem. Phys.* **1968**, *49*, 3465.
[35] D. Dixon, D. Zeroka, J. Wendoloski, Z. Wasserman, *J. Phys. Chem.* **1985**, *89*, 5334; C. J. Marsden, B. J. Smith, *J. Phys. Chem.* **1988**, *92*, 347.
[36] K. Kimura, K. Osafune, *Bull. Chem. Soc. Jpn.* **1975**, *48*, 2421; H. E. Van Wart, L. L. Shipman, H. A. Scheraga, *Acc. Chem. Res.* **1974**, *78*, 1848.
[37] C. O. Della Védova, J. J. P. Furlong, H.-G. Mack, *J. Mol. Struct.* **1994**, *317*, 165.

[38] C. O. Della Védova, *J. Raman Spectrosc.* **1989**, *20*, 729; C. O. Della Védova, *J. Raman Spectrosc.* **1989**, *20*, 483; C. O. Della Védova, E. L. Varetti, P. J. Aymonino, *Can. J. Spectrosc.* **1983**, *28*, 107.
[39] H.-G. Mack, C. O. Della Védova, H. Oberhammer, *J. Phys. Chem.* **1992**, *96*, 9215.
[40] C. O. Della Védova, *J. Raman Spectrosc.* **1989**, *20*, 581.
[41] M. F. Erben, C. O. Della Védova, R. M. Romano, R. Boese, H. Oberhammer, H. Willner, O. Sala, *Inorg. Chem.* **2002**, *41*, 1064.
[42] W. R. Cullen, D. C. Frost, D. Vroom, *J. Am. Chem. Soc*. **1969**, *8*, 1803; S. Lias, J. E. Bartmess, J. F. Liebman, J. L. Holmes, R. D. Levin, W. G. Mallard, *J. Phys. Chem. Ref. Data 17* **1988**, Suppl. No 1.

Received December 12, 2002